Veterinary Parasitology 191 (2013) 228–239



Veterinary Parasitology

journal homepage: www.elsevier.com/locate/vetpar

# Evidence of intracellular stages in *Trypanosoma* (*Megatrypanum*) *theileri* in non-phagocytic mammalian cells

Yen-Feng Lee[a,b], Ching-Chang Cheng[a], Jiun-Sheng Chen[a,b], Nai-Nu Lin[a,b], Yi-Wen Hung[a,b], Jiunn-Min Wang[c], Wu-Chun Tu[d], Kwong-Chung Tung[b,1], Yung-Tsung Chiu[a,e,*,1]

[a] *Department of Medical Education and Research, Taichung Veterans General Hospital, 160, Sec. 3, Taichung Harbor Road, Taichung 40705, Taiwan*
[b] *Department of Veterinary Medicine, National Chung-Hsing University, 250, Kuo-Kuang Road, Taichung 40227, Taiwan*
[c] *Department of Pathology and Laboratory Medicine, Taichung Veterans General Hospital, Taichung 40705, Taiwan*
[d] *Department of Entomology, National Chung-Hsing University, Taichung 40227, Taiwan*
[e] *Department of Animal Science, National Chung-Hsing University, Taichung 40227, Taiwan*

ARTICLE INFO

*Article history:*
Received 7 March 2012
Received in revised form 27 August 2012
Accepted 29 August 2012

*Keywords:*
*Trypanosoma theileri*
Intracellular stages
Autophagy
Lysosome
TGF-β

ABSTRACT

*Trypanosoma* (subgenus *Megatrypanum*) *theileri* was first identified over one hundred years ago, and is a widespread parasite in cattle. Its life cycle within the mammalian host has rarely been reported. Whether there is an intracellular stage in tissues is unknown and such a stage has not been demonstrated experimentally. Intriguingly, using Giemsa staining with light microscopy and transmission electron microscopy examination, we found that the parasite was able not only to attach to cells but also to invade several phagocytic and non-phagocytic mammalian cells. Based on these findings, we conducted further investigations using a special antibody in immunofluorescence confocal images. Moreover, we examined a series of possible events of cell invasion in *T. theileri*. The results revealed that GM1, a marker of membrane rafts, was implicated in the mechanism of entry by this parasite. After incubation with tissue culture trypomastigotes, the gelatinolytic activity was significantly increased and accumulated at the attachment sites. Using ultrastructural localization detection by CytoTracker live imaging and confocal immunofluorescence microscopy, we found that lysosome fusion and the autophagy pathway were engaged in invaginating processes. *T. theileri* amastigotes also invaded cells and were enclosed by the lysosomes. Furthermore, tissue-cultured trypomastigotes were found to be capable of triggering intracellular free $Ca^{2+}$ transients and TGF-β-signaling. Our findings that intracellular amastigote stages exist in mammalian cells infected with *T. theileri* and that the invasion processes involved various host cell components and cell signalings were extremely surprising and warrant further investigation.



## 1. Introduction

*Trypanosoma theileri* belongs to the subgenus *Megatrypanum*. It was first described in cattle by Theiler, Laveran and Bruce in 1902 (Hoare, 1972). This species is a cosmopolitan parasite of cattle and may occur with a high incidence. There is increasing evidence of immunosuppression involvement and association with a concomitant disease (Doherty et al., 1993). However, its life cycle is not fully understood. The vectors are Tabanidae and *Hyalomma anatolicum anatolicum*. *T. theileri* in tabanids is

* Corresponding author at: Department of Education and Research, Taichung Veterans General Hospital, 160, Sec. 3, Taichung Harbor Road, Taichung City 40705, Taiwan. Tel.: +886 4 23592525x4060; fax: +886 4 23592705.
*E-mail addresses:* leeyenf@yahoo.com.tw (Y.-F. Lee), chengjzvm@hotmail.com (C.-C. Cheng), roger894351@gmail.com (J.-S. Chen), nnlin@vghtc.gov.tw (N.-N. Lin), oldhjk@vghtc.gov.tw (Y.-W. Hung), jmwang@vghtc.gov.tw (J.-M. Wang), wctu@dragon.nchu.edu.tw (W.-C. Tu), kctung1@dragon.nchu.edu.tw (K.-C. Tung), ytchiu@vghtc.gov.tw (Y.-T. Chiu).

[1] These authors contributed equally to this work.

0304-4017 © 2012 Elsevier B.V. Open access under CC BY-NC-ND license.
http://dx.doi.org/10.1016/j.vetpar.2012.08.027

typically characterized by stercorarian transmission (Böse and Heister, 1993; Latif et al., 2004). An experimental rodent model has not been established.

The epimastigote and large trypomastigote forms can be revealed in peripheral blood. *T. theileri* may cause long-lasting cryptic infections with typically low parasitemia. The flagellates have also been found in extravascular sites of lymph nodes, kidney, spleen, and brain (Sudarto et al., 1990; Braun et al., 2002). The existence of intracellular stages of *T. theileri* in tissues has not been reported. Basically there are two life cycle types of trypanosomes with largely different pathogenic mechanisms and therapy strategies: (1) *T. brucei*, which lives in blood, is called Salivaria because of transmission by saliva and (2) *Trypanosoma cruzi*, which can invade cells and has an intracellular amastigote stage, is called Stercoraria because of transmission by feces. Although *T. theileri* characterized by stercorarian transmission has been described, no intracellular invasion similar to that of *T. cruzi* is known. Herein, we attempted to determine cell invasion by *T. theileri* using tissue culture-derived trypomastigotes (TCT) and extracellular amastigotes.

In general, the penetration of *T. cruzi* into host cells is achieved through a series of multi-step processes involving various molecules of the parasites and the host cell. Firstly, the parasites attach to the cell membrane, and then they are internalized by being surrounded by the parasitophorous vacuoles (PV). After escaping to the cytosol, differentiating into amastigotes and carrying out intracellular replication, the parasites finally transform into trypomastigotes and are released from the infected cell (Epting et al., 2010).

Initially, host cell cholesterol and specialized membrane rafts enriched in Monosialotetrahexosyl Ganglioside 1 (GM1) are requires for *T. cruzi* cell entry (Fernandes et al., 2007). Trypanosomatids elaborate a large array of peptidases, among which the cathepsin L-like (CATL) cysteine protease has been found in *T. theileri* (Rodrigues et al., 2010). The archetype of trypanosome CATL, named cruzipain, can promote parasite invasion of cardiovascular cells through inducing $Ca^{2+}$ signaling. Recently, matrix metalloproteinases (MMPs) have also emerged as a key regulator of *T. cruzi* infections (Nogueira de Melo et al., 2010). In addition, during invasion, lysosomes are recruited to the host plasma membrane in a calcium-signaling pathway-dependent manner (Rodríguez et al., 1996; Andrade and Andrews, 2004). Interestingly, *T. cruzi* utilizes an unusual metabolic pathway to accomplish invasion: induction of autophagy. Microtubule-associated protein 1 light chain 3 (MAP1LC3), an autophagosome marker, is highly co-localized at the parasite invasion site. Starvation or pharmacological induction of autophagic formation before *T. cruzi* infection significantly increased the number of infected cells, whereas inhibitors of this pathway reduced it (Romano et al., 2009). Ming et al. (1995) found that *T. cruzi* invasion of mammalian cells requires activation of the TGF-β signaling pathway, and administrating this cytokine exogenously greatly enhanced parasite internalization (Ming et al., 1995). Surprisingly, thus far a bona fide TGF-β from TCT has never been characterized. *T. cruzi* penetration into host cells also leads to intracellular $Ca^{2+}$ mobilization, both in trypanosome and target cells (Yoshida, 2006). $Ca^{2+}$transients are necessary for rapid rearrangements in the host cell cytoskeleton and recruitment of host cell lysosomes (Rodríguez et al., 1995, 1996). Experimentally buffering host cell intracellular free $Ca^{2+}$ or depleting intracellular $Ca^{2+}$ stores abrogated parasite invasion (Tardieux et al., 1994; Rodríguez et al., 1995).

The objective of the present study was to investigate whether *T. theileri* possesses intracellular amastigote stages in *in vitro* cells. If it can be proven, thereby the related molecular events of parasite-host cell interactions can be characterized and will also become the corroborating evidence for *T. theileri* cell invasion.

## 2. Materials and methods

### 2.1. Cells and parasites

A *T. theileri* TWTth1 strain was obtained from supernatants of infected BHK cells, as described in our previous study (Lee et al., 2010). Cultured trypanosomas were cryopreserved and the parasites were controlled under low culture passage, with no more than six passages through the entire experimental procedure. Amastigotes were generated in culture by incubating freshly harvested trypomastigotes in liver infusion tryptose medium containing 10% FBS (Invitrogen) at 37 °C in a humidified atmosphere of 5% $CO_2$ for 72 h. BHK (baby hamster kidney cell), SVEC4-10 (mouse lymph node endothelial cell), H9c2(2-1) (rat heart myoblast) and RAW 264.7 (mouse monocyte/macrophage cell) cell lines were obtained from the Bioresource Collection and Research Centre in the Food Industry Research and Development Institute (BCRC, FIRDI), Hsinchu, Taiwan, and were cultured according to the manufacturer's instructions. Tissue culture trypomastigotes (TCT) were obtained from the supernatants of infected BHK cells cultivated in Dulbecco's Modified Eagle Medium (DMEM) supplemented with 2% FBS. A pure suspension of TCT from a culture of infected BHK cells was obtained by collection and centrifugation of the medium at 3000 × *g* for 15 min. Highly motile trypomastigotes were then recovered following swimming up to the supernatant fraction for 3 h in DMEM at 37 °C in an atmosphere of 5% $CO_2$.

### 2.2. Light and electron microscopy observation

To ensure infectivity, trypanosome-infected culture cells were prewashed with phosphate-buffered saline (PBS) and fixed in methanol followed by Giemsa staining. Transmission and scanning electron microscopy (TEM, SEM) was used for examination, as previously described (Lee et al., 2010).

### 2.3. Cell attachment and invasion assays

For *T. theileri* attachment and invasion assays, the standardized procedure (Lima and Villalta, 1989) was modified in this study. BHK, H9c2, SVEC and RAW 264.7 cell lines (BCRC, FIRDI) were grown at 37 °C in 24-well plates containing $1 \times 10^5$ cells in DMEM with 10% FBS in an atmosphere of 5% $CO_2$. To measure attachment, cells were

infected with TCT at a proportion of 20:1 parasites/cell. After 1 h at 37 °C, the plates were washed four times with DMEM to remove non-adherent parasites. Under these conditions the parasite attaches to the host cells and minimal internalization occurs. For invasion assays, 3 h incubation at 37 °C was followed by re-incubation in fresh DMEM with 2% FBS for an additional 72 h to allow the differentiation of internalized parasites into amastigote forms, which are more easily quantified. Cells were immediately fixed with 4% paraformaldehyde (PFA) in PBS and stained with Giemsa. Interaction rates were determined by manual counting in a total of random 100 cells. The total number of parasites attached TCT per 100 cells and the percentage of cells containing attached parasites were calculated. In addition, intracellular parasites were counted to calculate the percentage of cell invasion.

### 2.4. Ganglioside GM1 labeling

After aldehyde fixation, cells were washed with PBS and then permeabilized with PGN solution (PBS, 0.15% gelatin, 0.1% sodium azide containing 0.1% saponin) for 15 min. Samples then underwent GM1 labeling by incubation with a 1 μg/ml cold solution of CTX-B – Alexa Fluor® 488 (Molecular Probes) for 30 min. Chamber slides were mounted in Vectashield mounting medium with 4′,6-diamidino-2-phenylindole (DAPI) and images were acquired on a confocal fluorescence microscope (Fernandes et al., 2007).

### 2.5. Detection of proteinase of T. theileri TWTth1

#### 2.5.1. PCR amplification and phylogenetic analysis of CATL genes

PCR amplifications of 477-bp DNA fragments, using oligonucleotide primers DTO154 and DTO155, corresponding to partial catalytic domains of CATL (cdCATL) enzymes were performed, as described previously (Cortez et al., 2009). The reactions were performed for 35 cycles at 94 °C (1 min), 56 °C (1 min), and 72 °C (1 min), followed by a final extension of 10 min at 72 °C. The sequence was confirmed by BLAST searches against the GenBank database at the National Center for Biotechnology Information, USA (http://blast.ncbi.nlm.nih.gov/Blast.cgi).

#### 2.5.2. Determination of metalloproteinase activity by gel zymography

For preparation of parasite soluble extract, three-day-old cultured pure TCT were harvested by centrifugation (3000 × *g*, 10 min, 4 °C) in order to clean any residual from culture medium components. The resulting pellets were sonicated in sterile PBS on ice with a microtip for two 15-s bursts at a setting of 2.5 (Sonics Vibra-Cell VCX 750). Unbroken cells and nuclei were removed by centrifugation at 10,000 × *g* for 10 min at 4 °C. The supernatant was then collected, aliquoted, and stored at −80 °C (Burleigh et al., 1997). The samples were diluted 1:10 in zymography sample buffer. The protein content of supernatants was determined by preparing bovine serum albumin (BSA) solution as the standard curve. Twenty μg of protein from each sample was run on 10% SDS-PAGE containing gelatin (1.0 mg/ml) without previous heating or reduction and electrophoresis was carried out at 4 °C at a constant voltage of 90 V. After electrophoresis, the gels were washed twice with 2.5% Triton X-100 (Sigma, USA) followed by overnight incubation at 37 °C with zymography $Ca^{2+}$ containing development buffer, pH 7.0. Finally, lytic bands were identified on substrate gel by staining with Coomassie Blue and the images were analyzed with a 1D Gel-Pro® analyzer.

#### 2.5.3. In situ zymography

To detect the loci of MMPs activity within invading H9c2 cells, an *in situ* zymography approach was employed (Galis et al., 1995). Briefly, after incubation with *T. theileri* for one hour, H9c2 cells were washed with PBS five times, and then incubated with DQ-labeled gelatin (Invitrogen) substrate solution (20 μg/ml DQ-gelatin, 50 mM Tris, pH 6.8, 50 mM NaCl, 20 mM $CaCl_2$) for 2 h at 37 °C in the dark. After the substrate solution was washed off, slides were incubated in 4% PFA for 10 min, washed with PBS, mounted with DAPI, and photographed with identical exposure settings using a laser confocal microscope (FV1000-D, Olympus).

### 2.6. Immunofluorescence double staining for laser confocal microscopy imaging

After fixation with 4% paraformaldehyde (PFA) in PBS for 5 min, chamber slides with attached cells were washed three times in PBS. Nonspecific immunoglobulin binding sites were blocked with 5% BSA for 30 min at room temperature, and then cells were incubated with first antibody: rabbit anti-TWTth1 polyclonal antibody, MAP1LC3A antibody (ab64123, Abcam), or TGF-β pan specific polyclonal antibody (AB-100-NA, R&D Systems) with Tris-buffered saline-Tween 20 (TBS-T) containing 2% BSA at 4 °C overnight. The sections were then incubated with FITC conjugated anti-rabbit IgG for 1 h at room temperature, followed by washing, mounting and examination by laser confocal microscopy.

### 2.7. Quantitation of gene expression by qRT-PCR

Analysis of transcripts of the TGF-β1 gene by quantitative real-time reverse transcription polymerase chain reaction (qRT-PCR) was performed as described in our previous study (Cheng et al., 2010).

### 2.8. Live-cell imaging experiments

For tracing in live cell images, BHK, SVEC, and H9c2 cells and *T. theileri* were labeled with CellTracker™ Probes (Molecular Probes™) for long-term tracing: LysoTracker Red DND-99/Green DND-26 (L-7528, L-7526), and MitoTracker Red CMXRos/Green FM (M-7512, M-7514) within 30 min according to the manufacturer's protocol (Invitrogen), followed by Hoechst 33342 (H-21492) staining for invasion assay.

### 2.9. Autophagy formation in infected H9c2 cells and parasite co-localization

To identify the possible interaction between *T. theileri* and the host cell *via* the autophagic pathway, two sets of experiments were performed. (A) After 3 h infection, cells were washed four times with PBS and fixed with 4% PFA for 10 min at room temperature. Autophagosomes were stained with anti-MAP1LC3 antibody as described in Section 2.6 above. (B) H9c2 cells were transfected *in vitro* with pSelect-LC3-GFP expression plasmid (psetz-gfplc3, InvivoGen) by jetPEI™ transfection reagent (PolyPlus Transfection), according to the instructions supplied by the manufacturer. For the *in vitro* infection assay, LC3-GFP-expressing H9c2 cells were plated onto an Ibidi 35 mm u-Dish (Ibidi, GmbH, Martinsried, Germany), at a density of $4 \times 10^3$ cells per well, and incubated overnight at 37 °C in a 5% $CO_2$ humidified atmosphere. Before infection, cells were washed once with culture medium to remove nonadhered cells. TCT were added at a parasite-to-host cell ratio of 5:1 and infection was carried out for 3 h at 37 °C. After incubation, Hoechst staining to label the nucleus and kinetoplasts was performed for 20 min. In addition, positive autophagy control was induced by washing grown cells three times with PBS and incubating them with starvation media (DMEM without FBS) at 37 °C for 24 h. During autophagosome formation, LC3-GFP is processed and recruited to the autophagosome membrane, where it can be imaged as cytoplasmic puncta by confocal fluorescence microscopy.

### 2.10. $Ca^{2+}$ signaling activities with invasion

Changes in $Ca^{2+}$ concentration were detected with the fluorescence probe Fluo-2/AM based on a modified version of a previously described protocol (Moreno et al., 1994). Briefly, H9c2 cells were plated for 48 h before the assay at $5 \times 10^3$ per dish, on a 35 mm glass bottom, and loaded with 5 mM fluo-2/AM (Molecular Probes Inc.) for 60 min at 37 °C in the dark. After loading, the dishes were washed in Hepes-buffered Ringer's solution. The cells on cover slips were then transferred to a microchamber on the stage of an inverted Olympus microscope, and viewed under bright light and UV illumination using a 40× oil immersion fluorescence objective. $Ca^{2+}$ concentration was monitored for 1 min at the basal level. Fluorescence images were collected with a video camera (CCD-C72; Dage/MTI, Michigan city, IN) through a 340 nm objective and recorded on an optical memory disk (TQ-3031F; Panasonic, Secaucus, NJ), at time-lapse intervals of 1 s using a computer-controlled shutter system (Photon Technology International; PTi Corp., Birmingham, NJ). $Ca^{2+}$ was monitored by alternating excitation wavelengths of between 340 nm and 380 nm and emission at 510 nm with a Delta Scan System (Photon Technology International; Princeton, NJ), and parasites were added to the cells at 50 s after initiation of the time-lapse recording. All the experiments were carried out at 30 °C.

### 2.11. Statistical analysis

All data are expressed as mean ± SD. Descriptive statistics were first used for analysis of normality. A Bonferroni *t*-test or a Mann–Whitney Rank Sum Test was used depending on the normality of data. The mean values of two groups were considered significantly different if $^{*}P < 0.05$, $^{**}P < 0.01$, or $^{***}P < 0.001$.

## 3. Results

### 3.1. T. theileri attached to mammalian cells by flagella and cell invasion

To ensure the initial step of invasion, parasite-infected culture cells were observed under light microscopy (Giemsa staining), TEM and SEM (Fig. 1). Parasites were strongly bound to the cell surface and could not be dislodged even with extensive washings with PBS. Because TCT is a pleomorphic population, different forms of trypomastigotes were found to be attached to the cells (Fig. 1A and B). In TEM images, *T. theileri* was attached to BHK cells (Fig. 1C). After infection of H9c2 cells, Giemsa staining showed that parasites had replicated inside the PV (Fig. 2A). The self-prepared mouse polyclonal antibody for

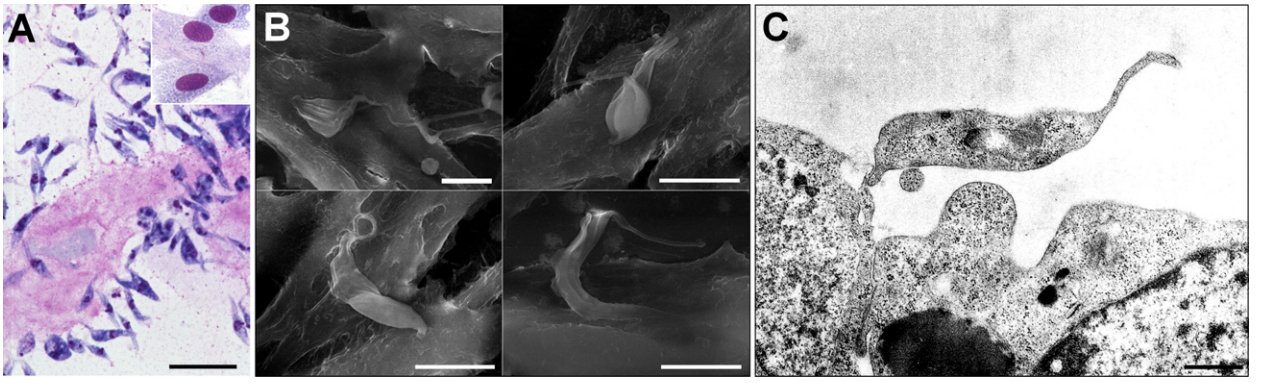


**Fig. 1.** BHK cells were infected with *T. theileri*. Parasites were attached to the cell surface. (A) Giemsa staining after 3 days of infection. bar = 20 μm. Upper right panel, BHK control cells. (B) SEM observation 3 h after infection. Different forms of parasites from the pleomorphic tissue culture-derived trypomastigotes (TCT) were attached to the feeder cells, bar = 5 μm. (C) TEM observation 3 h after infection, bar = 1.25 μm.

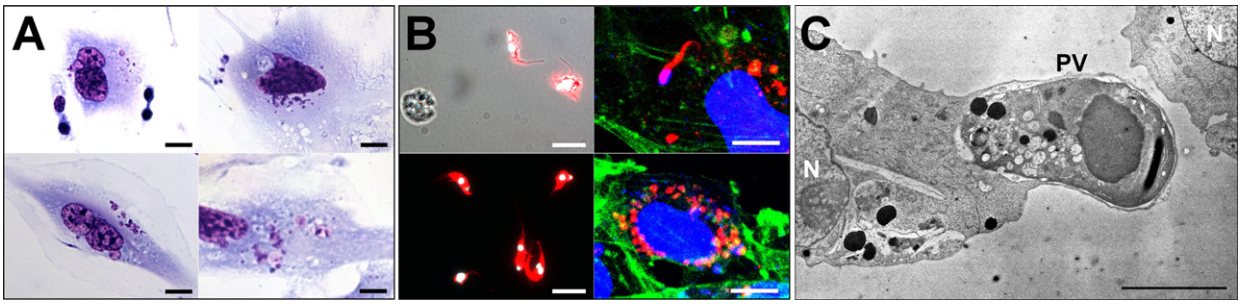


**Fig. 2.** Intracellular forms of *T. theileri* corresponding on day 5 after infection of H9c2 cells were investigated. Parasites multiplied inside the parasitophorous vacuole (PV), as revealed by Giemsa staining under light microscopy, bar = 20 μm (A). H9c2 cardiomyoblasts are indicated by actin staining (phalloidin, green); *T. theileri* was identified by indirect immunofluorescence using specific polyclonal antibody against TWTth1 (red). Parasites have a nucleus and a single large mitochondrion containing a kinetoplast (DAPI, blue), bar = 10 μm (B). TWTth1-infected H9c2 cells were observed under TEM. N: nucleus of an infected cell, PV: an intracellular parasitophorous vacuole, bar = 5 μm (C). (For interpretation of the references to color in the artwork, the reader is referred to the web version of the article.)

**Table 1**
*T. theileri* attachment and invasion assays.

| | BHK | H9c2 | SVEC | RAW 264.7 |
|---|---|---|---|---|
| Parasite-attached cell/100 cells | 64 ± 20*** | 72 ± 12*** | 19 ± 4 | 84 ± 6*** |
| Attached parasite No./100 cells | 115 ± 37*** | 209 ± 49*** | 24 ± 5 | 197 ± 21*** |
| Parasite-invaded cell/100 cells | 19 ± 7 | 27 ± 16*** | 12 ± 3 | 22 ± 11* |

Assays were done in triplicate independently, and experiments were repeated three times. The data represent the mean of triplicates ± standard deviation and the asterisks indicate statistically significant differences comparison with SVEC cell.
* $P < 0.05$.
*** $P < 0.001$.

*T. theileri* was specifically bound to TWTth1 including different forms (Fig. 2B, bottom left panel), but not to host cells (Fig. 2B, upper left panel, arrow). *T. theileri* were multiplied in the cytosol of H9c2 cells (Fig. 2B, right panels). The ultra-thin sections prepared for TEM examination revealed a large parasitophorous vacuole (PV) containing the parasite inside the cytosol of infected cardiomyocytes (Fig. 2C).

The results of *T. theileri* attachment assays in BHK, H9c2, SVEC and RAW 264.7 cells revealed 64 ± 20, 72 ± 12, 19 ± 4 and 84 ± 6 parasite-attached cells/100 cells, and 115 ± 37, 209 ± 49, 24 ± 5 and 197 ± 21 attached parasites/100 cells, respectively (Table 1). The numbers of parasite-attached cells and attached parasites were significantly higher in BHK, H9c2 and RAW 264.7 cells as compared with SVEC cells (Table 1, $P < 0.001$). In addition, the invasion assays showed 19 ± 7, 27 ± 16, 12 ± 3 and 22 ± 11 parasite-invaded cells/100 cells, respectively (Table 1). The invasion rate was significantly higher in H9c2 and RAW 264.7 cells than in SVEC cells ($P < 0.001$ and 0.05).

### 3.2. Raft marker GM1 is implicated in recruitment during *T. theileri* invasion

To determine whether *T. theileri* entry underlies membrane rafts of host cells, H9c2 cells were labeled with CTX-B. GM1 (green) enrichment was observed at the entry site

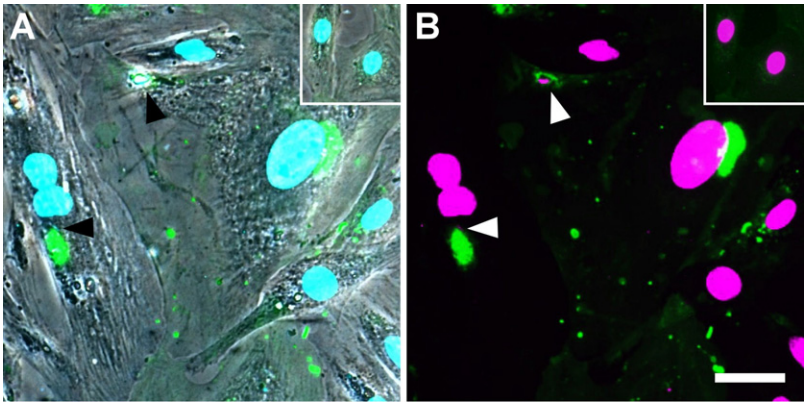


**Fig. 3.** Detection of ganglioside GM1 (green) using CTX-B labeling at the entry sites and in the PV during H9c2 cell invasion. (A) DAPI (indigo-blue) was merged with phase contrast DIC image. The nucleus and kinetoplast are labeled with DAPI. Parasites are stained as dots, corresponding to the nucleus and kinetoplast (arrowhead). (B) An invading parasite (arrowhead). DAPI (pink color) was merged with CTX-B (green), bar = 20 μm. Upper right panel, H9c2 control cells. (For interpretation of the references to color in the artwork, the reader is referred to the web version of the article.)

of the plasma membrane around infected TCT (Fig. 3A and B, arrowheads). In contrast, GM1 enrichment was not observed in non-infected control H9c2 cells (Fig. 3A and B, upper right panel).

### 3.3. PCR amplification and phylogenetic analysis of CATL genes of T. theileri isolates

According to a recent study, the CATL sequence fragment is highly suitable as the target for phylogenetic analysis in *T. theileri* (Rodrigues et al., 2010). We therefore sequenced this gene of Taiwan *T. theileri* isolates as previously described (Cortez et al., 2009). Phylogenetic analyses revealed the sequence of TWTth1 trypanosomes was clustered within the clade of the *T. theileri* lineage TthIB genotype. Its sequence was completely identical with NCBI GenBank accession numbers of genes: GU299391.1, GU299394.1, GU299397.1, GU299399.1, and GU299400.1, with length 477, identities 477/477 (100%) and gaps 0/477 (0%), among the TthIB lineage.

### 3.4. T. theileri demonstrated MMP-like activity in situ and in gel zymography

After TCTs were added to H9c2 cells, the gelatinolytic activity was significant increased and accumulated in the body of *T. theileri* and at the attachment site of the cell membrane (Fig. 4B–D, arrowheads). In contrast, gelatinolytic activity was only present at the adjacent cell junction in the control (Fig. 4A). Gelatin gels were incubated with TCT lysates of *T. theileri*, unwashed parasites (Fig. 4E, lane 1) and washed twice with PBS (Fig. 4E, lane 2). The gel contained prominent activity revolving in a molecular mass of approximately 65 kDa, the only visible activity on the gel (Fig. 4E).

### 3.5. Lysosome fusion during cell invasion by T. theileri trypomastigotes or amastigotes

Lyso-Tracker Red pre-stained H9c2 (Fig. 5A–C) or SVEC cells (Fig. 5D and E) were inoculated with TCTs (Fig. 5A, upper right panel) and amastigotes (Fig. 5D, upper right panel) for 24 h. Confocal laser scanning images corresponding to the stack of serial confocal sections and a larger magnification of one single-plane section is shown. TCTs stain as two dots, corresponding to the nucleus and kinetoplast in Hoechst stain, and were co-localized with lysosomes in Lyso-Tracker pre-stained H9c2 cells (Fig. 5A, arrowhead) 24 h after inoculation. Furthermore, the Mito-Tracker-labeled TCTs partially invaded the H9c2 cytosol (colocalized with Lyso-Tracker) as early as 3 h post-infection (Fig. 5B), with marked entry at 24 h (Fig. 5C). The mitochondria, which showed high activity in the amastigote stage, were analyzed and also labeled with Mito-Tracker during invasion of SVEC cells by *T. theileri*. TWTth1 amastigotes, identified by small Hoechst dots, were co-localized with the lysosomes in Lyso-Tracker pre-stained SVEC cells 24 h after inoculation (Fig. 5D, arrowhead). Mito-Tracker pre-stained amastigotes were also found to be surrounded by lysosomes in Lyso-Tracker pre-stained SVEC cells at 3 h post-infection (Fig. 5E, arrowhead). Taken together, the observations described above provide evidence that the invading parasites co-localize with lysosomes, as seen in the merged image, indicating TCTs and amastigotes of *T. theileri* are fused with lysosomes in H9c2 and SVEC cell invasion.

### 3.6. Autophagosome formation in infected H9c2 cells and parasite colocalization

First, endogenous autophagosomes were detected by indirect immunofluorescence using MAP1LC3 antibody in TCT-infected H9c2 cells. The parasites were detected by

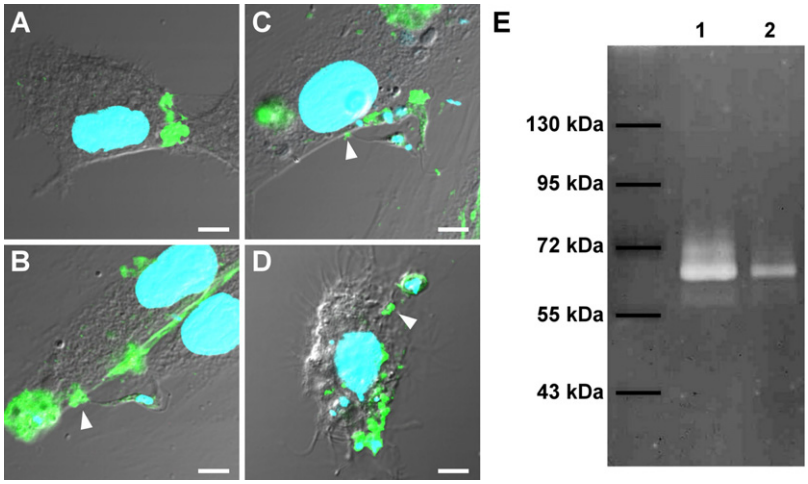


**Fig. 4.** Gelatinolytic activity: *in situ* (A–D) and in gels (E). (A) *In situ* gelatinolytic activity (green) was only present at the adheral cell junction in control H9c2 cells. After incubation with TCTs (B and C) or extracellular amastigotes (D), the gelatinolytic activity was significantly increased and accumulated on the body of *T. theileri* and at the invasion sites (arrowheads). DAPI, indigo-blue color. bar = 20 μm. (E) Gelatinolytic activities (~65 kDa) of TCT lysates were detected in gelatin gel. Unwashed (lane 1) and washed parasites (lane 2) are parts of the same gel incubated for 18 h at pH 7.0, 37 °C. (For interpretation of the references to color in the artwork, the reader is referred to the web version of the article.)

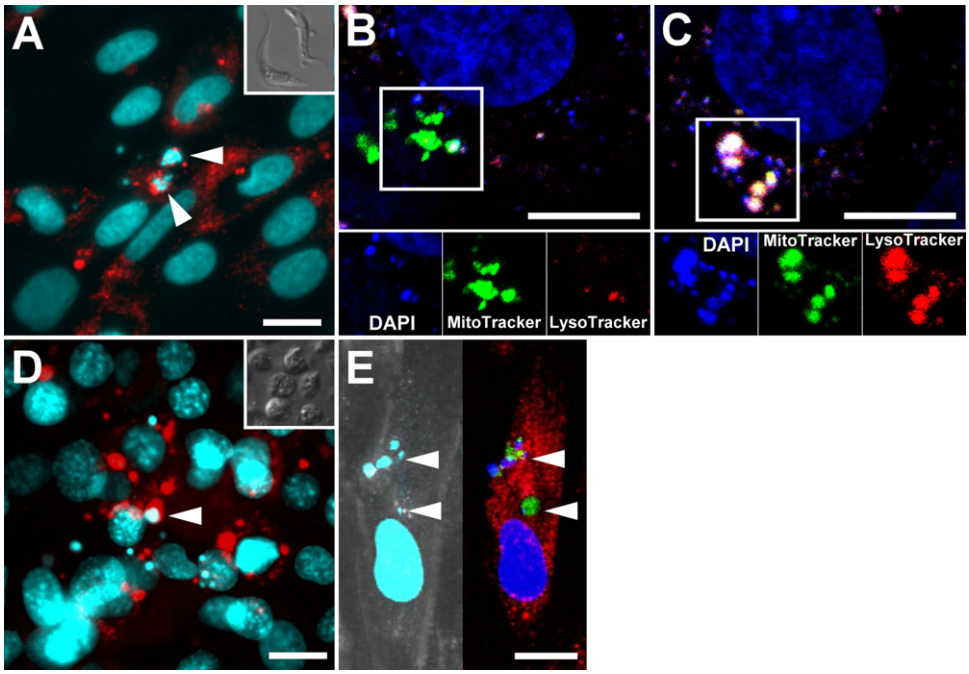


**Fig. 5.** Lyso-Tracker trace *T. theileri* invasion. Lyso-Tracker pre-stained H9c2 cells (A–C) and SVEC cells (D and E) were inoculated with TCTs (A, upper right panel) and amastigotes (D, upper right panel) for 3 h (B, E) and 24 h (A, C, D). Lyso-Tracker (red) was merged with Hoechst stain (nucleus and kinetoplast) in infected H9c2 cells (A). Mito-Tracker-labeled TCTs partially invaded into the H9c2 cytosol (colocalized with Lyso-Tracker) at 3 h post-infection (B), marked entry at 24 h (C). In Lyso-Tracker-pre-stained SVEC cells, TWTth1 amastigotes (D, arrowhead, small Hoechst dots) were markedly colocalized with the lysosome 24 h after inoculation. An early image at 3 h post-infection (E) shows that phase contrast merged with Hoechst (E, left) and Mito-Tracker-pre-stained amastigotes (green) merged with Lyso-Tracker (red) (E, right). The arrowheads indicate to TCT or amastigotes invading the cells, which are inside a vacuole traced by Lyso-Tracker. (A–D) bar = 10 μm, (E) bar = 20 μm. (For interpretation of the references to color in the artwork, the reader is referred to the web version of the article.)

labeling the nucleus and kinetoplast with DAPI (Fig. 6A, arrowhead) that were surrounded by the protein LC3 (Fig. 6B, green), indicating its association in invasion. As compared to the H9c2 control cell (Fig. 6A and B, upper right panel), the LC3 protein was not present. Second, Fig. 6C revealed that pSelect-LC3-GFP-transfected H9c2 cells expressed a stable and strong positive control image after starvation. Three hours after infection, anti-TWTth1 antibody confirmed TCTs (Fig. 6D and E, red parasite body with DAPI-labeled nucleus and kinetoplast) were colocalized with the protein LC3 (autophagosome), indicating that the *T. theileri* parasitophorous vacuole (PV) is not just a consequence of protein expression (Fig. 6D and E). These results demonstrated a more intensive interaction between autophagosomes and *T. theileri* at the invasion sites than was previously thought.

### 3.7. *T. theileri engaged TGF-β for invasion and induction of TGF-β expression in H9c2 cells*

Basal TGF-β protein expression levels are shown in the control H9c2 cells (Fig. 7A). TWTth1-infected H9c2 cells revealed significant TGF-β protein expression at the penetration sites (Fig. 7B, red) and merged with the TWTth1 body (Fig. 7B, small DAPI dots). Quantitative RT-PCR showed that *T. theileri* infection significantly increased TGF-β1 mRNA of infected host cells ($P = 0.025$) (Fig. 7C).

### 3.8. *Cytosolic $Ca^{2+}$ concentration increased in both parasite and host cells after TWTth1 inoculation*

Calcium signaling showed onset of $Ca^{2+}$ transients 3 h after *T. theileri* infection using Fura-2/AM staining under confocal microscopy (Fig. 8A). TWTth1 inoculation significantly increased the cytosolic $Ca^{2+}$ concentration at the attachment site (Fig. 8A, arrowhead). Quantification of $Ca^{2+}$ oscillations of Fura-2/AM-loaded H9c2 cells was immediately performed after TWTth1 inoculation from zero to 35 min. Time-lapse images of $Ca^{2+}$ changes from TWTth1 infected cells and non-infected control are shown in Fig. 8B. In the experiments described here the kinetics of cytosolic free $Ca^{2+}$ changes demonstrated a slight increase at 5 min, a significant rise starting at 10 min ($P < 0.01$), and lasting for more than 35 min ($P < 0.001$) after addition (Fig. 8C).

## 4. Discussion

In the present study, we provide evidence that *T. theileri* is able to invade mammalian cells in a series of processes that involve gelatinolytic MMPs, membrane rafts, autophagy, a lysosome pathway, as well as $Ca^{2+}$ and TGF-β-signaling.

*In vitro*, *T. theileri* can be isolated in hemoculture from cattle blood. Several cell-free media permit *T. theileri* growth; a wide variety of mammalian cells have also been utilized for first isolation and consequent propagation.

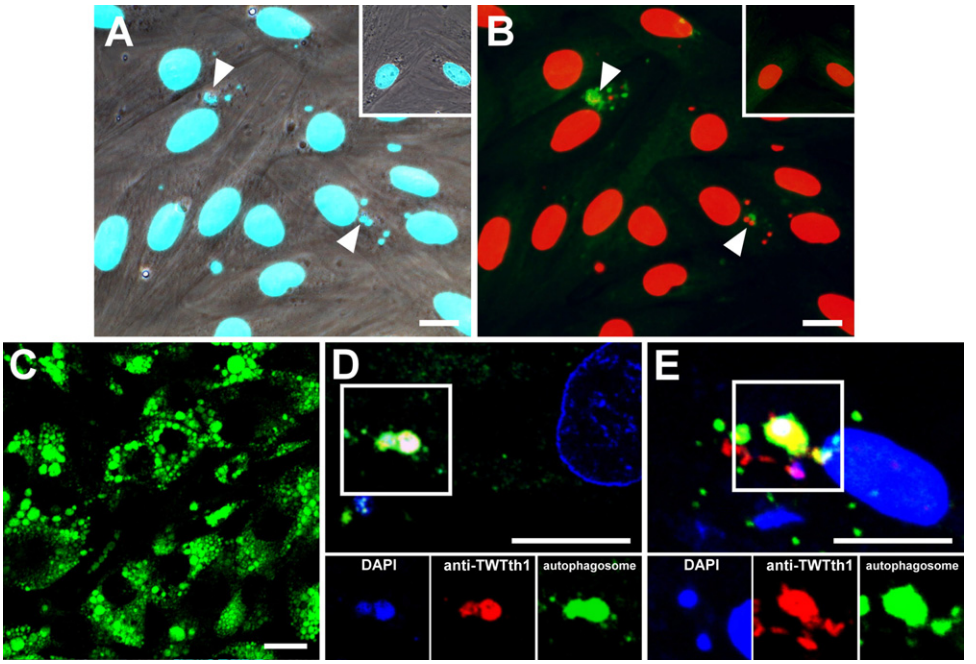


**Fig. 6.** Autophagy formation in TWTth1 invasion. After 3 h infection, the parasites were detected by labeling the nucleus and kinetoplast with DAPI (arrowhead) which shows phase contrast images were merged (A). The endogenous LC3 was examined by MAP1LC3 immunostaining in infected H9c2 cells (B, green), and DAPI (red color) were merged, bar = 10 μm (B). The upper right panel in A and B shows the H9c2 control cells. pSelect-LC3-GFP-transfected H9c2 cells induced LC3 expression by starving, as a strong positive control, autophagosomes (green), bar = 20 μm (C). The transfected H9c2 cells were inoculated with TCTs for 3 h, followed by specific TWTth1 detection using a mouse polyclonal antibody against *T. theileri* (red), bar = 10 μm (D, E). (For interpretation of the references to color in the artwork, the reader is referred to the web version of the article.)

Intriguingly, without these feeder-layer cells there is no long-term survival (Rodrigues et al., 2003). *T. theileri* TCTs are often attached to culture cells and often by their posterior ends (Wink, 1979). Therefore, we were especially interested in whether *T. theileri* would be able to invade the host cells, not just attach to them. According to previous reports, some clinical evidence implicated *T. theileri* as an intracellular parasite. First, amastigotes have been found within primary bovine spleen phagocytic cells following 18 days in culture. However, the possibility that it was just a simple phagocytic phenomenon cannot be excluded (Moulton and Krauss, 1972). Second, a latently infected cattle experiment indicated the parasite was associated with lymphocytes (Griebel et al., 1989). Third, *T. theileri* has been found in cerebrospinal fluid (Braun et al., 2002). Nevertheless, whether it is able to cross the blood–brain barrier into the brain or not remains unknown. Finally, given its ability to infect transplacentally, it is capable of transferring *via* blood vessels possibly by direct invasion through endothelium. In order to examine cell invasion, four kinds of cells were used in this study: BHK (baby hamster kidney cell), SVEC4-10 (mouse lymph node endothelial cell),

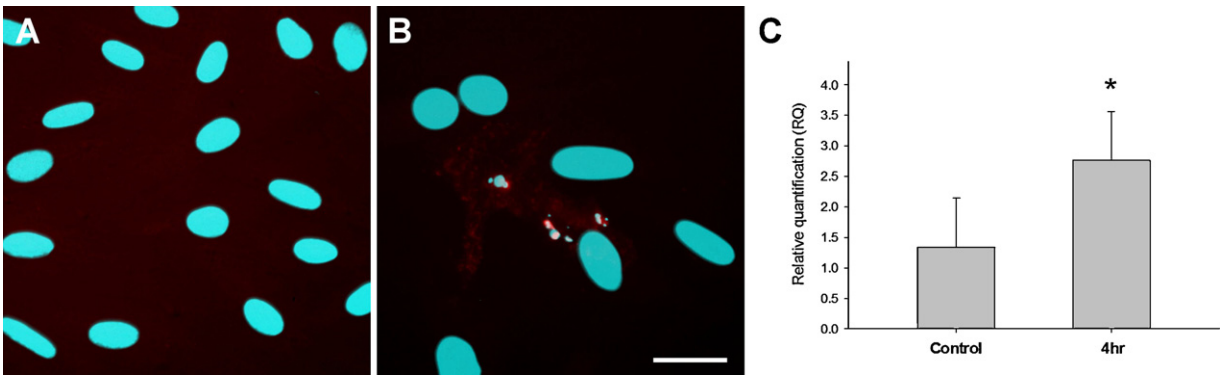


**Fig. 7.** TGF-β expression in *T. theileri* infection. (A) H9c2 control cells and (B) TWTth1-infected H9c2 cells revealed significant TGF-β expression at the penetration site by anti-pan TGF-β staining (red), combined with DAPI (the nucleus and kinetoplast). Bar = 50 μm. (C) *T. theileri* infection significantly increased TGF-β1 mRNA expression levels in infected host cells. A representative trace of 5 independent experiments that were conducted on 3 separate preparations is shown, $^{*}P = 0.025$. (For interpretation of the references to color in the artwork, the reader is referred to the web version of the article.)

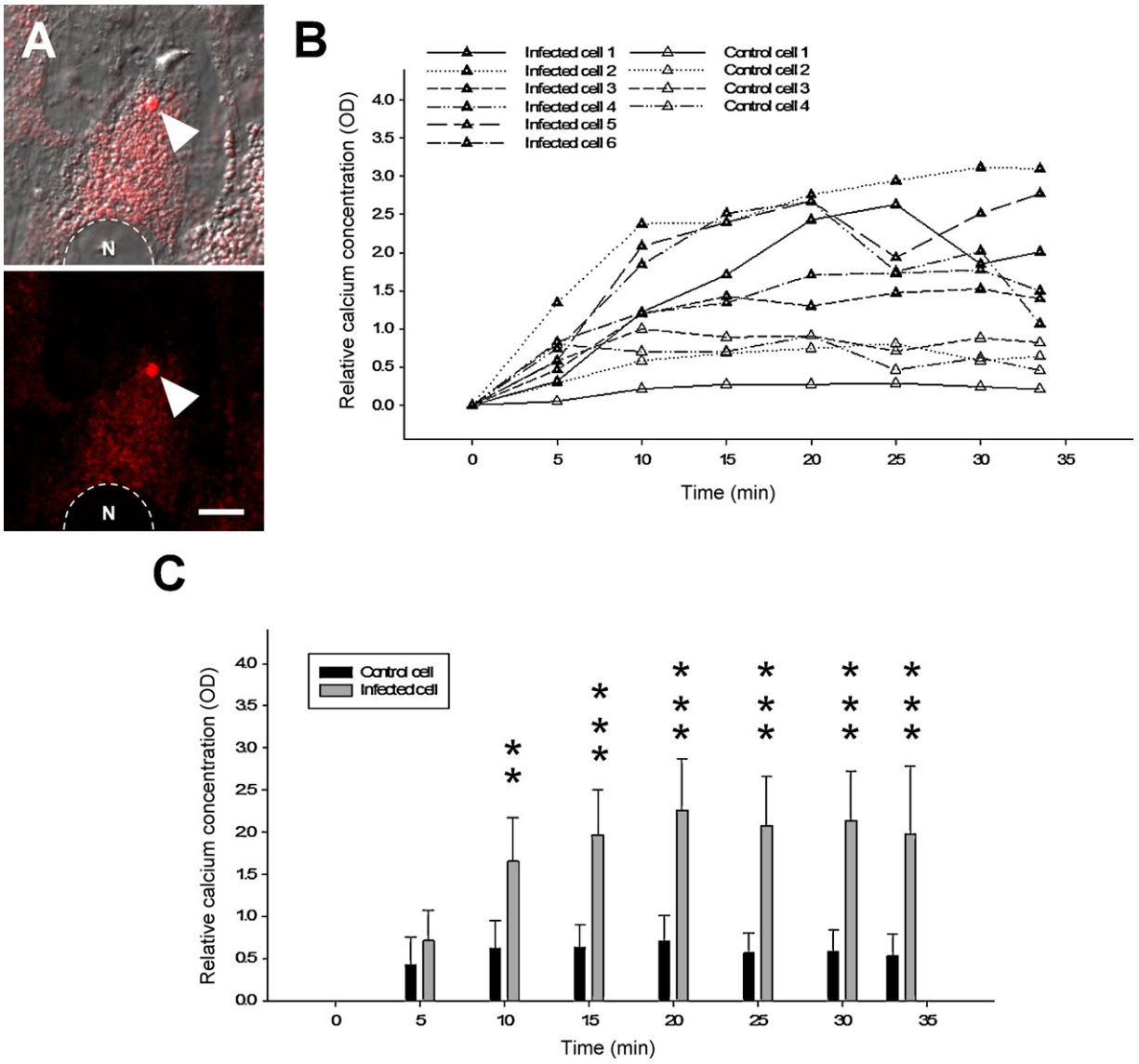


**Fig. 8.** Calcium signaling after TWTth1 inoculation. (A) $Ca^{2+}$ Fura-2 staining under confocal microscopy. The cytosolic $Ca^{2+}$ concentration was significantly increased at the attachment site (arrowhead). (B–C) The quantification of $Ca^{2+}$ oscillations of H9c2 in response to infection in time-lapse fluorescence microscopy. Fura-2/AM-loaded H9c2 cells were mounted on a recording chamber, and 25–40 regions of interest representing individual cells were selected. Cells were exposed to TCTs ($10^5$ parasites/ml) in HBSS at the starting point, and exposure lasted to the end of the 35-min observation period. $^{**}P < 0.01$, $^{***}P < 0.001$.

H9c2(2-1) (rat heart myoblast) and RAW 264.7 (mouse monocyte/macrophage cell) cell lines.

Experimentally, culture-derived metacyclic trypomastigotes have been generally accepted as a model for insect vector-derived metacyclic trypomastigotes, invasion of mammalian cells. In addition another important form, extracellular amastigotes, prematurely released from infected cells or generated by the extracellular differentiation of TCTs, can also infect cultured cells and animals in *T. cruzi* (Ley et al., 1988).

Most importantly, we provide direct evidence for invasion of *T. theileri* into host cells, multiplication and completion of its life cycle in host cells like those of *T. cruzi*. Extracellular free parasites could be detected at 5–7 days after infection. In an attachment assay, a previous study showed that when *T. theileri* were cultured together with vertebrate monolayer cell lines, about 50–70% of the trypanosomes were closely associated with the cells (Wink, 1979). In this study, attachment rates ranged from 19% to 84% (Table 1). The invasion rates of *T. theileri* gained about 20%, which were similar to those of *T. cruzi* in the study by Rodríguez et al. (1996), but lower than those in the study by Rubin-de-Celis et al. (2006) (40%). Although the reason for this disparity is unclear and needs to be addressed, the attachment and invasion rates of SVEC were significantly lower than those of other cell lines.

Even though no experimental rodent model has been established, in order to investigate *T. theileri* invasion *in vivo* we tried to establish such a model. Unfortunately, we observed no clinical signs, pathologic changes or deaths (data not shown).

To date, development of vaccines against trypanosomes has mainly involved exploring candidate antigens which are expressed on the surface of the parasite. Several molecules of *T. cruzi* have been hypothesized to interact with the host cells, including gp30, gp 35/50, penetrin (gp60), gp63, gp82, gp83, gp85, gp90, mucins/trans-sialidase, secreted sialidase (SAPA), mucin p45, cruzipain, oligopeptidase B, casein kinase II substrate (TC1), LYT1 protein and prolyl oligopeptidase (POP). It is known that some of them can bind to specific receptors present in the host cell; for example, cytokeratin 18, laminin, galectin-3, fibronectin, integrins, sialic acid, TGF-β receptor, bradykinin receptors, nerve growth factor receptors (TrkA and TrkC), toll-like receptors and low density lipoprotein receptors (review by de Souza et al., 2010; Nagajyothi et al., 2011). Nevertheless, thus far no surface molecules of *T. theileri* have been identified.

Besides the above mentioned molecules, caveolae and lipid rafts in the host cell membrane have also been shown to take part in *T. cruzi* invasion. The host cell GM1 ganglioside, a marker for lipid rafts, is enriched at the invasion site. Experimentally, colocalization between a specific GM1 probe (CTX-B) and an intracellular parasite suggest a participation of membrane rafts in the trypomastigote internalization. Pre-treatment with agents to disrupt membrane rafts significantly interfered with the adhesion of trypomastigotes to the macrophage surface (Fernandes et al., 2007; Barrias et al., 2007). Herein, lipid rafts enrichment in the early stage of invasion was first revealed in *T. theileri*. However, further blockage experiments are required to reconfirm this interaction effect.

Cathepsin L-like (CATL) cysteine proteases play crucial functions in differentiation, multiplication and infectivity in trypanosomes. Cruzipain activates bradykinin signaling to promote $Ca^{2+}$ release from endoplasmic reticulum (Scharfstein et al., 2000). CatL-like isoforms of *T. cruzi* (cruzipain), which is the archetype of a multigene family, have been described in *T. b. brucei* (brucipain), *T. b. rhodesiense* (rhodesain), *T. congolense* (congopain), and *T. rangeli* (rangelipain) (Scharfstein et al., 2000). Cluster analysis of *T. theileri* CATL sequences from Taiwan (TWTth1 isolates) revealed they are identical with other genes among the TthIB lineage including the TthIB genotype from Brazil and the USA. Given these findings, we postulate that internal transit of livestock and cattle materials may be an important factor in this phylogeographic relationship. A recent report revealed isolates in Thailand cattle were characterized by an unexpectedly large polymorphic genetic repertoire distinct from that of other countries (Garcia et al., 2011). Due to limitations in the sample size, we could not assess the phylogenetic diversity in Taiwan.

To the best of our knowledge, this is the first time that a fluorescently-labeled gelatin was used as substrate for *in situ* zymography in a trypanosomide study. The apparent gelatinase activity was shown at the attachment site of the cell membrane (Fig. 4B–D). In our experience, this could be considered as an excellent method for evaluating *in situ* invasion. Although TCT lysates of *T. theileri* exhibited prominent activity in gelatin gel zymography (Fig. 4E), the genes, biochemical characterizations and bio-functions of *T. theileri*-metalloproteinases will need more extensive study.

Native or recombinant glycoproteins gp82, gp83, gp30, gp35/50 on the membrane surface and oligopeptidase B of *T. cruzi* are able to trigger a transient increase in intracellular $Ca^{2+}$ in host cells (Epting et al., 2010). In contrast, non-infective epimastigotes are not capable of inducing $Ca^{2+}$ signaling (Tardieux et al., 1994). According to previous studies and our study, after living TCT were added to the chamber, $Ca^{2+}$ increase occurred within a few seconds in individual cells. Furthermore, our result indicated the *T. theileri* infective group was statistically significant at 10 min (Fig. 8B and C), which is roughly consistent with earlier *T. cruzi* data that at least 10 min of trypomastigote-host cell interaction were required for the invasion process (Tardieux et al., 1994).

Lysosome recruitment to the plasma membrane of host cells was required for *T. cruzi* invasion (Tardieux et al., 1992; Albertti et al., 2010). Trypomastigotes triggering calcium flux can promote transient rearrangement of the cells' peripheral actin cytoskeleton and induce the microtubule/kinesin-mediated transport and fusion of lysosomes to the plasma membrane. After that, *T. cruzi* uses this membrane to form a PV (Rodríguez et al., 1996, 1999). Experimentally, the kinetics of lysosomal marker accumulation and their subsequent loss indicates escape of parasites into the cytoplasm. According to our observation, *T. theileri* was housed in the lysosome vacuole during the first 3 h, then became more visible at 24 h, a finding which is similar to the results of previous studies of *T. cruzi* (Rodríguez et al., 1996; Andrade and Andrews, 2004). Our further observation indicated *T. theileri* ultimately disappeared at 72 h.

The autophagic response may function as a defense against pathogens, but in some cases the microorganism "hijacks" this cellular process to infect the host cell. Recently, Romano et al. described the recruitment of autophagosomes to facilitate parasite entry and enhance *T. cruzi* invasion. And intriguingly, a high expression of LC3 was observed to be induced by the parasite itself (Romano et al., 2009). In this study we have provided the first evidence that autophagosomes are recruited to the *T. theileri* PV (Fig. 6). Given these findings, we suggest this pathway may be implicated in trypanosomatide invasion. Experimentally, GFP-LC3 is a widely used and useful tool for visualizing the time-series maturation process of autophagosomes. Notably, the accumulation of GFP-LC3 puncta *in vitro* does not rule out the possibility that they are induced in autophagosome-independent situations such as protein aggregation and detergent treatment (Kuma et al., 2007; Ciechomska and Tolkovsky, 2007). Thus, direct detection of endogenous LC3 by immunostaining, and further electron microscopy analysis are preferred for monitoring autophagy.

Some authors have proposed that *T. cruzi* is capable of activating latent host TGF-β (Ming et al., 1995; Waghabi et al., 2005). Some proteases secreted by the

parasite might activate latent TGF-β-associated extracellular components (Araújo-Jorge et al., 2008). The exposure of phosphatidylserine on the surface of *T. cruzi* subverts the microbicidal function of macrophages by inducing the TGF-β signaling pathway, thereby favoring the survival of trypomastigotes in macrophages (Damatta et al., 2007). This study is the first to provide striking evidence that *T. theileri* induces host cell TGF-β1 expression during cell invasion.

Collectively, our results support the observation that *T. theileri* tends to be clustered as a cell invasion trypanosome whose process is highly similar to that of *T. cruzi*. These findings strongly imply evolutionary conservation in cell invasion among these ancient eukaryotes. Because *T. theileri* is not harmful to humans, it could be a powerful model for trypanosomide cell invasion.

## Conflicts of interest

All authors have read and approved the final manuscript. The authors declare that they have no competing interests.

## Authors' contributions

Y.-F.L. conceived the study, carried out the design, data acquisition and analysis and drafted the manuscript. C.-C.C. participated in the design of the study and performed data acquisition and analysis. J.-S.C., N.-N.L. and Y.-W.H. provided the experimental facility support and participated in the statistical analysis. J.-M.W. interpreted the data and helped to draft the manuscript. W.-C.T. participated in the electron microscopy examination. K.-C.T. and Y.-T.C. participated in the conception, design and coordination of the study, and made a critical revision of the manuscript for important intellectual content.

## Acknowledgements

This work was support by grants from Taichung Veterans General Hospital (TCVGH -1007309C, -1006506C). Technical support provided by the hospital's Precision Instrument Center is gratefully acknowledged.

## References

Albertti, L.A., Macedo, A.M., Chiari, E., Andrews, N.W., Andrade, L.O., 2010. Role of host lysosomal associated membrane protein (LAMP) in *Trypanosoma cruzi* invasion and intracellular development. Microb. Infect. 12, 784–789.

Andrade, L.O., Andrews, N.W., 2004. Lysosomal fusion is essential for the retention of *Trypanosoma cruzi* inside host cells. J. Exp. Med. 200, 1135–1143.

Araújo-Jorge, T.C., Waghabi, M.C., Soeiro Mde, N., Keramidas, M., Bailly, S., Feige, J.J., 2008. Pivotal role for TGF-beta in infectious heart disease: the case of *Trypanosoma cruzi* infection and consequent Chagasic myocardiopathy. Cytokine Growth Factor Rev. 19, 405–413.

Barrias, E.S., Dutra, J.M., De Souza, W., Carvalho, T.M., 2007. Participation of macrophage membrane rafts in *Trypanosoma cruzi* invasion process. Biochem. Biophys. Res. Commun. 363, 828–834.

Böse, R., Heister, N.C., 1993. Development of *Trypanosoma* (*Megatrypanum*) *theileri* in tabanids. J. Eukaryot. Microbiol. 40, 788–792.

Braun, U., Rogg, E., Walser, M., Nehrbass, D., Guscetti, F., Mathis, A., Deplazes, P., 2002. *Trypanosoma theileri* in the cerebrospinal fluid and brain of a heifer with suppurative meningoencephalitis. Vet. Rec. 150, 18–19.

Burleigh, B.A., Caler, E.V., Webster, P., Andrews, N.W., 1997. A cytosolic serine endopeptidase from *Trypanosoma cruzi* is required for the generation of $Ca^{2+}$ signaling in mammalian cells. J. Cell Biol. 136, 609–620.

Ciechomska, I.A., Tolkovsky, A.M., 2007. Non-autophagic GFP-LC3 puncta induced by saponin and other detergents. Autophagy 3, 586–590.

Cheng, C.C., Lin, N.N., Lee, Y.F., Wu, L.Y., Hsu, H.P., Lee, W.J., Tung, K.C., Chiu, Y.T., 2010. Effect of Shugan-huayu powder, traditional Chinese medicine, on hepatic fibrosis in rat model. Chin. J. Physiol. 53, 223–233.

Cortez, A.P., Rodrigues, A.C., Garcia, H.A., Neves, L., Batista, J.S., Bengaly, Z., Paiva, F., Teixeira, M.M., 2009. Cathepsin L-like genes of *Trypanosoma vivax* from Africa and South America—characterization, relationships and diagnostic implications. Mol. Cell Probes 23, 44–51.

Damatta, R.A., Seabra, S.H., Deolindo, P., Arnholdt, A.C., Manhaes, L., Goldenberg, S., de Souza, W., 2007. *Trypanosoma cruzi* exposes phosphatidylserine as an evasion mechanism. FEMS Microbiol. Lett. 266, 29–33.

de Souza, W., de Carvalho, T.M., Barrias, E.S., 2010. Review on *Trypanosoma cruzi*: host cell interaction. Int. J. Cell Biol. 2010, pii, 295394.

Doherty, M.L., Windle, H., Voorheis, H.P., Larkin, H., Casey, M., Clery, D., Murray, M., 1993. Clinical disease associated with *Trypanosoma theileri* infection in a calf in Ireland. Vet. Rec. 132, 653–656.

Epting, C.L., Coates, B.M., Engman, D.M., 2010. Molecular mechanisms of host cell invasion by *Trypanosoma cruzi*. Exp. Parasitol. 126, 283–291.

Fernandes, M.C., Cortez, M., Geraldo Yoneyama, K.A., Straus, A.H., Yoshida, N., Mortara, R.A., 2007. Novel strategy in *Trypanosoma cruzi* cell invasion: implication of cholesterol and host cell microdomains. Int. J. Parasitol. 37, 1431–1441.

Galis, Z.S., Sukhova, G.K., Libby, P., 1995. Microscopic localization of active proteases by in situ zymography: detection of matrix metalloproteinase activity in vascular tissue. FASEB J. 9, 974–980.

Garcia, H.A., Kamyingkird, K., Rodrigues, A.C., Jittapalapong, S., Teixeira, M.M., Desquesnes, M., 2011. High genetic diversity in field isolates of *Trypanosoma theileri* assessed by analysis of cathepsin L-like sequences disclosed multiple and new genotypes infecting cattle in Thailand. Vet. Parasitol. 180, 363–367.

Griebel, P.J., Gajadhar, A.A., Babiuk, L.A., Allen, J.R., 1989. *Trypanosoma theileri* associated with T-lymphocytes isolated from a latently infected cow. J. Protozool. 36, 415–421.

Hoare, C.A., 1972. The Trypanosomes of Mammals: A zoological Monograph. Blackwell Scientific Publications, Oxford, UK, pp. 123–141.

Kuma, A., Matsui, M., Mizushima, N., 2007. LC3, an autophagosome marker, can be incorporated into protein aggregates independent of autophagy: caution in the interpretation of LC3 localization. Autophagy 3, 323–328.

Latif, A.A., Bakheit, M.A., Mohamed, A.E., Zweygarth, E., 2004. High infection rates of the tick Hyalomma anatolicum anatolicum with *Trypanosoma theileri*. Onderstepoort J. Vet. Res. 71, 251–256.

Lee, Y.F., Cheng, C.C., Lin, N.N., Liu, S.A., Tung, K.C., Chiu, Y.T., 2010. Isolation of *Trypanosoma* (*Megatrypanum*) *theileri* from dairy cattle in Taiwan. J. Vet. Med. Sci. 72, 417–424.

Ley, V., Andrews, N.W., Robbins, E.S., Nussenzweig, V., 1988. Amastigotes of *Trypanosoma cruzi* sustain an infective cycle in mammalian cells. J. Exp. Med. 168, 649–659.

Lima, M.F., Villalta, F., 1989. T*rypanosoma cruzi* trypomastigote clones differentially express a parasite cell adhesion molecule. Mol. Biochem. Parasitol. 33, 159–170.

Ming, M., Ewen, M.E., Pereira, M.E., 1995. Trypanosome invasion of mammalian cells requires activation of the TGF beta signaling pathway. Cell 82, 287–296.

Moreno, S.N., Silva, J., Vercesi, A.E., Docampo, R., 1994. Cytosolic-free calcium elevation in *Trypanosoma cruzi* is required for cell invasion. J. Exp. Med. 180, 1535–1540.

Moulton, J.E., Krauss, H.H., 1972. Ultrastructure of *Trypanosoma theileri* in bovine spleen culture. Cornell. Vet. 62, 124–137.

Nagajyothi, F., Weiss, L.M., Silver, D.L., Desruisseaux, M.S., Scherer, P.E., Herz, J., Tanowitz, H.B., 2011. *Trypanosoma cruzi* utilizes the host low density lipoprotein receptor in invasion. PLoS Negl. Trop. Dis. 5, e953.

Nogueira de Melo, A.C., de Souza, E.P., Elias, C.G., dos Santos, A.L., Branquinha, M.H., d'Avila-Levy, C.M., dos Reis, F.C., Costa, T.F., Lima, A.P., de Souza Pereira, M.C., Meirelles, M.N., 2010. Detection of matrix metallopeptidase-9-like proteins in *Trypanosoma cruzi*. Exp. Parasitol. 125, 256–263.

Rodrigues, A.C., Campaner, M., Takata, C.S., Dell' Porto, A., Milder, R.V., Takeda, G.F., Teixeira, M.M., 2003. Brazilian isolates of *Trypanosoma* (*Megatrypanum*) *theileri*: diagnosis and differentiation of isolates from cattle and water buffalo based on biological characteristics and randomly amplified DNA sequences. Vet. Parasitol. 116, 185–207.

Rodrigues, A.C., Garcia, H.A., Ortiz, P.A., Cortez, A.P., Martinkovic, F., Paiva, F., Batista, J.S., Minervino, A.H., Campaner, M., Pral, E.M., Alfieri, S.C., Teixeira, M.M., 2010. Cysteine proteases of *Trypanosoma* (*Megatrypanum*) *theileri*: cathepsin L-like gene sequences as targets for phylogenetic analysis, genotyping diagnosis. Parasitol. Int. 59, 318–325.

Rodríguez, A., Martinez, I., Chung, A., Berlot, C.H., Andrews, N.W., 1999. cAMP regulates $Ca^{2+}$-dependent exocytosis of lysosomes and lysosome-mediated cell invasion by trypanosomes. J. Biol. Chem. 274, 16754–16759.

Rodríguez, A., Rioult, M.G., Ora, A., Andrews, N.W., 1995. A trypanosome-soluble factor induces IP3 formation, intracellular $Ca^{2+}$ mobilization and microfilament rearrangement in host cells. J. Cell Biol. 129, 1263–1273.

Rodríguez, A., Samoff, E., Rioult, M., Chung, A., Andrews, N.W., 1996. Host cell invasion by trypanosomes requires lysosomes and microtubule/kinesin-mediated transport. J. Cell Biol. 134, 349–362.

Romano, P.S., Arboit, M.A., Vázquez, C.L., Colombo, M.I., 2009. The autophagic pathway is a key component in the lysosomal dependent entry of *Trypanosoma cruzi* into the host cell. Autophagy 5, 6–18.

Rubin-de-Celis, S.S., Uemura, H., Yoshida, N., Schenkman, S., 2006. Expression of trypomastigote trans-sialidase in metacyclic forms of *Trypanosoma cruzi* increases parasite escape from its parasitophorous vacuole. Cell Microbiol. 8 (December (12)), 1888–1898.

Scharfstein, J., Schmitz, V., Morandi, V., Capella, M.M., Lima, A.P., Morrot, A., Juliano, L., Müller-Esterl, W., 2000. Host cell invasion by *Trypanosoma cruzi* is potentiated by activation of bradykinin B(2) receptors. J. Exp. Med. 192, 1289–1300.

Sudarto, M.W., Tabel, H., Haines, D.M., 1990. Immunohistochemical demonstration of *Trypanosoma evansi* in tissues of experimentally infected rats and a naturally infected water buffalo (*Bubalus bubalis*). J. Parasitol. 76, 162–167.

Tardieux, I., Nathanson, M.H., Andrews, N.W., 1994. Role in host cell invasion of *Trypanosoma cruzi*-induced cytosolic-free $Ca^{2+}$ transients. J. Exp. Med. 179, 1017–1022.

Tardieux, I., Webster, P., Ravesloot, J., Boron, W., Lunn, J.A., Heuser, J.E., Andrews, N.W., 1992. Lysosome recruitment and fusion are early events required for trypanosome invasion of mammalian cells. Cell 71, 1117–1130.

Waghabi, M.C., Keramidas, M., Feige, J.J., Araújo-Jorge, T.C., Bailly, S., 2005. Activation of transforming growth factor beta by *Trypanosoma cruzi*. Cell Microbiol. 7, 511–517.

Wink, M., 1979. *Trypanosoma theileri*: in vitro cultivation in tsetse fly and vertebrate cell culture systems. Int. J. Parasitol. 9, 585–589.

Yoshida, N., 2006. Molecular basis of mammalian cell invasion by *Trypanosoma cruzi*. An. Acad. Bras. Cienc. 78, 87–111.